

Viscous Flow and Jump Dynamics in Molecular Supercooled Liquids: I Translations

Cristiano De Michele¹ and Dino Loporini^{1,2} [*]

¹ Dipartimento di Fisica, Università di Pisa, V.Buonarroti, 2 I-56100 Pisa, Italy

² Istituto Nazionale di Fisica della Materia, Unità di Pisa

(Received July 22, 2021)

The transport and the relaxation properties of a molecular supercooled liquid on a isobar is studied by molecular dynamics. The molecule is a rigid heteronuclear diatomic system. The diffusivity is fitted over four orders of magnitude by the power law $D \propto (T - T_c)^{\gamma_D}$ with $\gamma_D = 1.93 \pm 0.02$ and $T_c = 0.458 \pm 0.002$. The self-part of the intermediate scattering function $F_s(k_{max}, t)$ exhibits a step-like behavior at the lowest temperatures. On cooling, the increase of the related relaxation time τ_α tracks the diffusivity, i.e. $\tau_\alpha \propto (k_{max}^2 D)^{-1}$. At the lowest temperatures fractions of highly mobile and trapped molecules are evidenced. Translational jumps are evidenced. The duration of the jumps exhibits a distribution. The distribution of the waiting-times before a jump takes place $\psi(t)$ is exponential at higher temperatures. At lower temperatures a power-law divergence is evidenced at short times, $\psi(t) \propto t^{\xi-1}$ with $0 < \xi \leq 1$ which is ascribed to intermittency. The shear viscosity is fitted by the power law $\eta \propto (T - T_c)^{\gamma_\eta}$ with $\gamma_\eta = -2.20 \pm 0.03$ at the lowest temperatures. At higher temperatures the Stokes-Einstein fits the data if *stick* boundary conditions are assumed. The product $D\eta/T$ increases at lower temperatures and the Stokes-Einstein relation breaks down at a temperature which is close to the one where the intermittency is evidenced by $\psi(t)$. A precursor effect of the breakdown is observed which manifests as an apparent stick-slip transition.

PACS numbers: 64.70.Pf, 02.70.Ns, 66.20.+d , 66.10.-x

I. INTRODUCTION

The relaxation phenomena and the transport properties of supercooled liquids and glassy materials are topics of current interest [1,2]. It is well known that, on approaching the glass transition temperature T_g from above, diffusion coefficients and relaxation times exhibit remarkable changes of several orders of magnitude which are under intense experimental, theoretical and numerical investigation. In the high-temperature regime the changes usually track the shear viscosity η in the sense that, if X denotes the diffusivity or the inverse of a relaxation time, the product $X\eta/T$ is nearly temperature-independent. In particular, both the Stokes-Einstein, $D \approx kT/6\pi\eta a$, and the Debye-Stokes-Einstein laws, $D_r \approx kT/\eta a^3$ are found to work nicely, D , D_r and a being the translational and the rotational diffusivity and the molecular radius, respectively. Differently, in deeply supercooled regimes there is wide evidence that the product *increases on cooling* evidencing the breakdown of the hydrodynamic behavior at molecular level and the decoupling by the viscous flow [3–6] [7–15].

Several models suggest that the decoupling between microscopic time scales and the viscous flow is a signature of the heterogeneous dynamics close to the glass transition, i.e. a spatial distribution of transport and relaxation properties [16–19]. Interesting alternatives are provided by frustrated lattice gas models [20] and the “energy landscape” picture [2,21–24]. Most interpretations suggest the existence of crossover temperatures below which a change of relaxation mechanism must occur

[3]. These temperatures are broadly found around $1.2T_g$, i.e. in the region where the critical temperature T_c predicted by the mode-coupling theory of the glass transition (MCT) is found [25]. Recent extensions of MCT for the shear viscosity to take into account current-fluctuations in addition to density fluctuations are reported [26].

During the last years molecular dynamics simulations (MD) proved to be a powerful tool to investigate supercooled liquids (for a recent review see ref. [27]). To date, MD studies investigated decoupling phenomena in atomic pure liquids [24] and atomic binary mixtures [28–33]. Most MD studies confirmed that the decoupling is due to dynamic heterogeneities [28,30–34]. In fact, “active” [31] or “mobile” [34] regions which largely contribute to set the macroscopic average value have been identified. In such regions hopping processes, enhancing the transport with respect to the hydrodynamic behavior, have been evidenced [28,31]. The occurrence of jumps in glasses has been reported several times in the recent past [29,35–37].

We are not aware of MD studies of the decoupling, and, more generally, of dynamic heterogeneities in *molecular* systems. This motivated the present and the following paper [38] to investigate the transport and the relaxation in a three-dimensional, one-component, molecular system. This is an important feature since most experimental work is carried out on that class of materials. In particular, the decoupling of microscopic relaxation from the viscous flow will be addressed in the light of the increased role played by the hopping processes. The present paper is limited to the translational degrees of

freedom whereas the following paper [38] deals with the rotational degrees of freedom.

The paper is organized as follows. In Sec. II the model and the details of the simulation are presented. The results concerning both single-particle and collective properties are discussed in Sec. III. The main conclusions are summarized in Sec. IV.

II. MODEL AND DETAILS OF SIMULATION

The system under study is a diatomic molecular liquid. The model has been extensively investigated to test the MCT predictions [39–41]. The atoms A and B of each molecule have mass m and are spaced by d . Atoms on different molecules interact via the Lennard-Jones potential:

$$V_{\alpha\beta}(r) = 4\epsilon_{\alpha\beta} \left[\left(\frac{\sigma_{\alpha\beta}}{r} \right)^{12} - \left(\frac{\sigma_{\alpha\beta}}{r} \right)^6 \right], \quad \alpha, \beta \in \{A, B\} \quad (1)$$

The potential was cutoff and shifted at $r_{cutoff} = 2.5\sigma_{AA}$. Henceforth, reduced units will be used. Lengths are in units of σ_{AA} , energies in units of ϵ_{AA} and masses in units of m . The time unit is $\left(\frac{m\sigma_{AA}^2}{\epsilon_{AA}} \right)^{1/2}$, corresponding to about $2ps$ for the Argon atom. The pressure P , temperature T and shear viscosity η are in units of $\epsilon_{AA}/\sigma_{AA}^3$, ϵ_{AA}/k_B and $\sqrt{m\epsilon_{AA}/\sigma_{AA}^2}$, respectively.

The model parameters in reduced units are: $\sigma_{AA} = \sigma_{AB} = 1.0$, $\sigma_{BB} = 0.95$, $\epsilon_{AA} = \epsilon_{AB} = 1.0$, $\epsilon_{BB} = 0.95$, $d = 0.5$, $m_A = m_B = m = 1.0$. The σ_{AA} and σ_{BB} values were chosen to avoid crystallization. The sample has $N = N_{at}/2 = 1000$ molecules which are accommodated in a cubic box with periodic boundary conditions. The viscosity was evaluated by using samples of $N = 108$ molecules.

We examined the isobar at $P = 1.5$ by the following procedure. First, the sample was equilibrated in isothermal-isobaric conditions. for a time t_{eq} t_{eq} was at least one order of magnitude longer the time needed by the self-part of the intermediate scattering function evaluated at the maximum of the static structure factor to become smaller than 0.1. In this step the equations of motion were integrated by using the RATTLE algorithm with Nosè-Andersen constant temperature and pressure dynamics [42]. The algorithm is detailed in Appendix A. The starting conditions of the equilibration run make the total momentum of the system to vanish and locate the center of mass at the center of the box. The Nosè-Andersen Lagrangian ensures that the center-of-mass position and the total momentum will not change during the run.

The data were collected in a production run in micro-canonical conditions. Integration was carried out by the RATTLE algorithm. The δt step ranges from 0.001 at higher temperatures to 0.004 at lower ones in the production run. The temperatures we investigated are $T =$

6, 5, 3, 2, 1.4, 1.1, 0.85, 0.77, 0.70, 0.632, 0.588, 0.549, 0.52, 0.5. The characterization of the system at $T = 0.77$ was limited to the diffusivity and the viscosity. The density at $T = 0.5$ was 0.6998 and decreased of a factor of about three at the highest temperatures. To check that thermal hystory is negligible, at least two independent equilibrations were performed and the subsequent production runs compared at the lowest temperatures.

III. RESULTS AND DISCUSSION

The section discusses the results of the study. First, we characterize the static properties of the system, i.e. the radial distribution function of the center-of-mass $g(r)$ and the static structure factor $S(k)$. Then, the single-particle and the collective dynamical properties of the system will be presented.

A. Static properties

The radial distribution function of the center of mass $g(r)$ is defined as:

$$g(r) = \frac{1}{4\pi N\rho r^2} \sum_{i \neq j} \langle \delta(|\mathbf{R}_i(0) - \mathbf{R}_j(0) - \mathbf{r}|) \rangle \quad (2)$$

ρ is the average density and $\mathbf{R}_i(t)$ is the position of the center of mass of the i -th molecule at time t . Representative plots of $g(r)$ at different temperatures are shown in Fig. 1. The pattern is typical of a disordered system. At $T = 0.5$, $g(r)$ exhibits the maximum at $r \cong 1.2$ and the minimum at $r \cong 1.6$. On increasing the temperature, the peaks broaden and shift at higher r values. The shoulder which is observed at $r \cong 1.1$ at the lowest temperatures has been already observed [43] and may be ascribed to local “T-shaped” or cross configurations of the molecules [44].

The static structure factor $S(k)$ is defined as

$$S(k) = \frac{1}{N} \langle \rho_k \rho_{-k} \rangle \quad (3)$$

ρ_k is the Fourier transform of the density. Representative plots of $S(k)$ at different temperatures are shown in fig. 1.

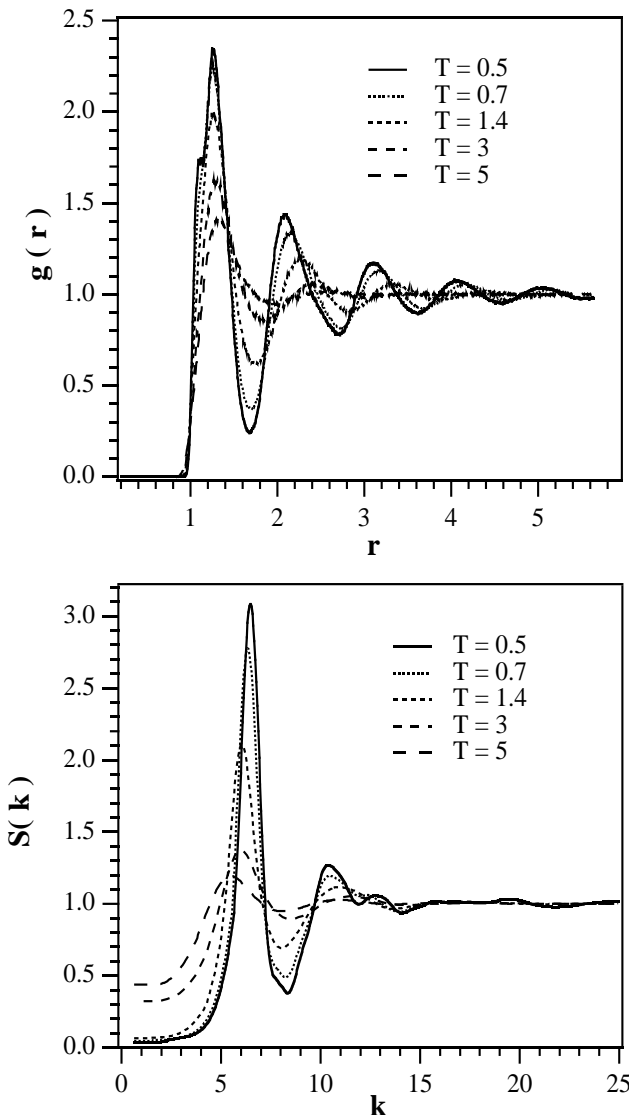


FIG. 1. Radial distribution function $g(r)$ (top) and static structure factor $S(k)$ (bottom) of the molecular center of mass for selected temperatures.

The above results rule out possible crystallizations of the sample. This is anticipated by the absence of anomalies in the temperature dependence of the density. Direct inspection of several snapshots of the molecular configurations also supported the conclusion and did not reveal any orientational (liquid-crystalline) order. The absence of orientational order was also evidenced by the long-time behaviour of the rotational correlation function [38].

B. Single-particle dynamics

The section will discuss the single-particle dynamics. At short time scales one quantity of interest is the velocity self-correlation function of the center of mass :

$$C_{vv}(t) = \frac{1}{N} \sum_{i=1}^N \langle \mathbf{v}_i(t) \cdot \mathbf{v}_i(0) \rangle \quad (4)$$

$\langle A(t) \rangle$ denotes a proper time average of $A(t)$. Fig. 2 plots C_{vv} for different temperatures.

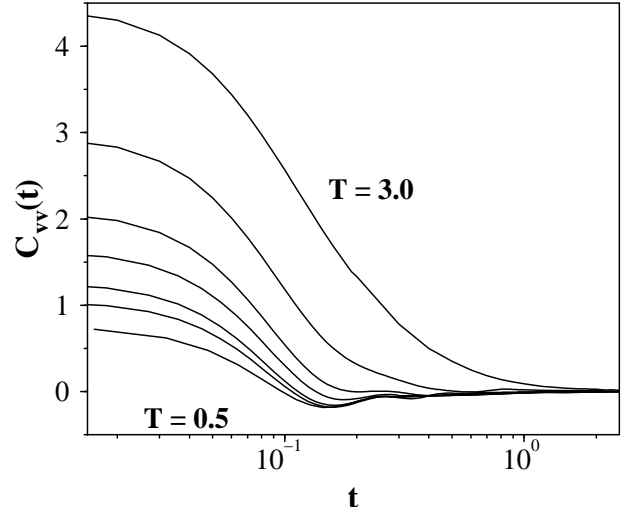


FIG. 2. Velocity self-correlation function of the center of mass. The curves refer to $T = 3, 2, 1.4, 1.1, 0.85, 0.7, 0.5$.

At very short times $C_{vv}(t) \cong \langle v^2 \rangle (1 - \langle \Omega^2 \rangle t^2/2 + \dots)$, where $\langle \Omega^2 \rangle$ is the Einstein frequency [44]. At the lower temperatures the damped oscillatory motion of the molecule inside the cage where it is accommodated becomes apparent. The effect signals that on a short time scale the supercooled liquid behaves as a solid.

The mean squared displacement of center of mass, $R(t)$ provides a first view of the translational motion of the molecules at intermediate and long time scales. It is defined as:

$$R(t) = \frac{1}{N} \sum_{i=1}^N \langle |\mathbf{R}_i(t) - \mathbf{R}_i(0)|^2 \rangle. \quad (5)$$

Plots of $R(t)$ at different temperatures are shown in fig.3. At short times the motion is ballistic and $R(t) \propto t^2$. At intermediate times $R(t)$ exhibits a crossover regime which is strongly temperature dependent. At higher temperature it reduces to a knee joining the ballistic and the diffusive regimes. At lower temperatures the molecule is effectively trapped inside the cage of the first neighbours and $R(t)$ exhibits a plateau. At long times the motion is diffusive and $R(t) = 6Dt$ where D is the diffusion constant.

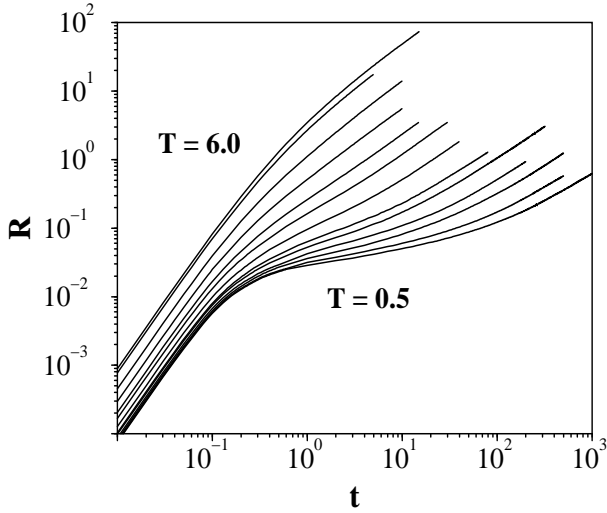


FIG. 3. Mean squared displacement of molecular center-of-mass $R(t)$ for all the temperatures under investigation but $T = 0.77$.

The occurrence of oscillatory motion during trapping is shown explicitly in fig.4 where the mean squared displacement and the velocity correlation function are compared at $T = 0.5$. The plot evidences that velocity correlations got lost within the lifetime of the cage.

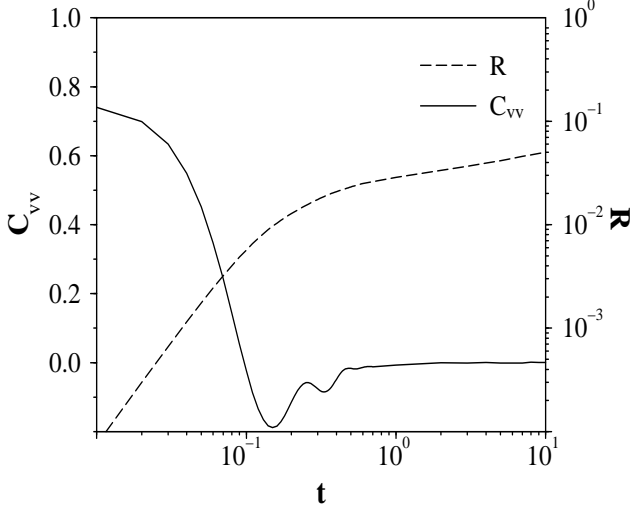


FIG. 4. Comparison of the mean squared displacement $R(t)$ and the velocity correlation function $C_{vv}(t)$ at $T = 0.5$. The onset of the damped oscillations takes place at the beginning of the plateau of $R(t)$: the molecule is colliding with the cage of the first neighbours.

The translational diffusion coefficient D is evaluated by the Einstein relation [42,44]:

$$D = \lim_{t \rightarrow \infty} \frac{R(t)}{6t} \quad (6)$$

In Fig. 5 the temperature dependence of D is shown. The plot emphasizes the scaling property of D which is nicely described over four decades by the power law :

$$D = C_D (T - T_c)^{\gamma_D} \quad (7)$$

Theoretical justification of eq.7 is provided by MCT [25]. In particular, the ideal MCT predicts the inequality $\gamma_D > 1.5$. Our best fit values are $\gamma_D = 1.93 \pm 0.02$ and $T_c = 0.458 \pm 0.002$, $C_D = 0.0481 \pm 0.0004$. For the same diatomic system with $N = 500$ and $P = 1$ it was found $\gamma_D = 2.2$ and $T_c = 0.475$ [39].

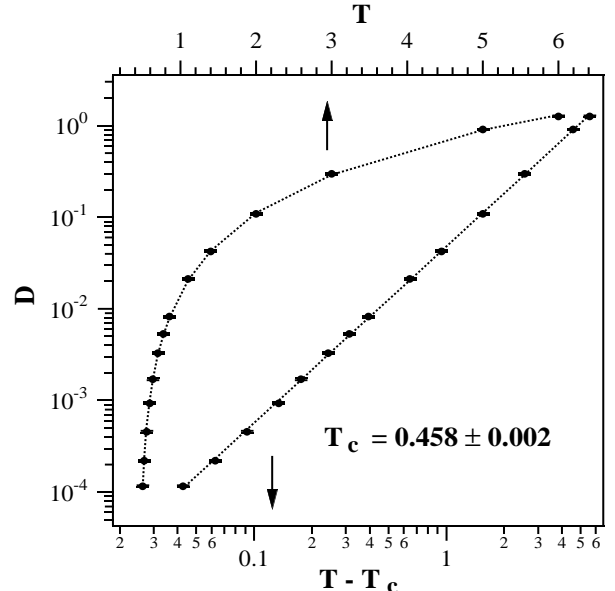


FIG. 5. Temperature dependence of the translational diffusion coefficient D . The dashed line is a fit with the power law eq.7 with $\gamma_D = 1.93 \pm 0.02$, $T_c = 0.458 \pm 0.002$ and $C_D = 0.0481 \pm 0.0004$.

It must be noted that at lower temperatures the above power law is expected to underestimate the diffusion coefficient [41]. The larger diffusivity with respect to the ideal MCT prediction close to T_c is not surprising. According to this approach, density-density correlations do not vanish at long times below T_c leading to a divergence of D at T_c . The extended MCT points out that hopping processes provide an effective mechanism to relax the density fluctuations at long time and make the diffusivity finite close to T_c . This point will be explicitly discussed later.

To characterize further the single-particle dynamics we evaluated the self-part of the intermediate scattering function :

$$F_s(k, t) = \langle \exp[i\mathbf{k} \cdot (\mathbf{R}_j(t) - \mathbf{R}_j(0))] \rangle \quad (8)$$

In fig. 6 $F_s(k, t)$ is plotted for all the temperatures we investigated at $k = k_{max}$. k_{max} is the position of the main peak of the static structure factor $S(k)$ at temperature T . We note that $F_s(k, t)$ always decays to zero and is independent of the thermal history of the sample (i.e. independent runs lead to the same result) signaling the equilibration of the sample. At higher temperatures the

decay is virtually exponential at long times, whereas at lower temperatures a two-step decay is observed.

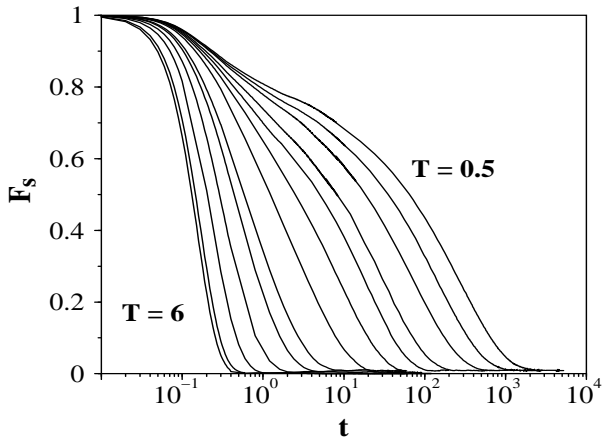


FIG. 6. Self-part of the intermediate scattering function $F_s(k_{max}, t)$. The curves refer to all the temperatures under investigation but $T = 0.77$.

The plateau which is observed at lower temperatures in $F_s(k_{max}, t)$ is due to the trapping of the molecules. This is seen by comparing fig.3 with fig.6. Precise predictions on the scaling features of the plateau of $F_s(k_{max}, t)$ are made by MCT [25]. A thorough comparison for the present model is found in ref. [41].

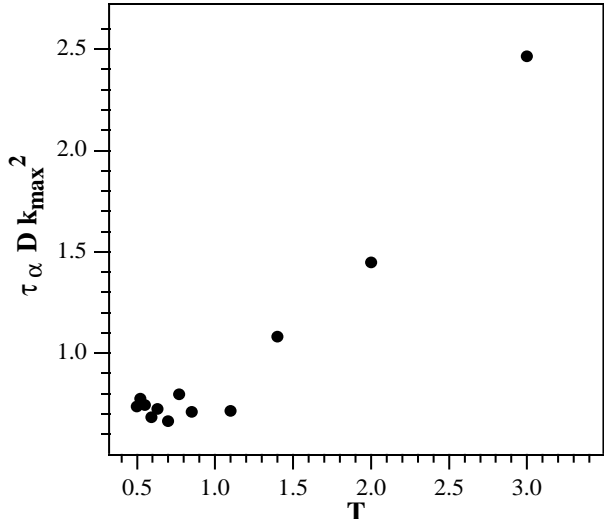


FIG. 7. Temperature dependence of the product $\tau_\alpha D k_{max}^2$.

At longer times the cage where the molecule is trapped opens and the density-density correlations vanish. The long-time decay of $F_s(k_{max}, t)$ is well fitted by the stretched exponential $A \exp(-t/\tau)^\beta$. Stretching is appreciable at lower temperatures ($\beta_{0.5} = 0.677$) and becomes negligible ($\beta \approx 1$) for $T > 0.85$.

The knowledge of $F_s(k_{max}, t)$ offers the opportunity to investigate the time scale of structural relaxation being usually denoted by the α -relaxation time τ_α . We

have evaluated it by the condition $F_s(k_{max}, \tau_\alpha) = 1/e \approx 0.3679$. At low temperatures a nice fit is provided by $\tau_\alpha = C_\alpha(T - T_c)^{\gamma_\alpha}$, being T_c the same best-fit value drawn by the diffusivity. The best fit value of the exponent is $\gamma_\alpha = -1.89 \pm 0.05$ which is quite close to $\gamma_D = 1.93$. Diffusive motion in simple liquids leads to the exponential decay of $F_s(k, t)$ with time costant $\tau = 1/Dk^2$ [44]. Even the decay at long times is better described by a stretched exponential, the approximate equality $\gamma_\alpha \approx \gamma_D$ prompted us to investigate the temperature dependence of the product $\tau_\alpha D k_{max}^2$. The results are shown in fig.7. For $T < 1.1$ the product approaches the constant value 0.72 ± 0.05 . In this range τ_α and D change of more than two orders of magnitude. Alternative definitions of τ_α , e.g. involving the area below $F_s(k_{max}, t)$ do not affect significantly the result. Removing the k_{max}^2 term results in slightly poorer fit. The k^2 scaling of the primary relaxation time τ_k^s , evaluated as the area below $F_s(k, t)$, was already noted in the hard sphere system at the critical packing fraction in the region $1.5 \leq ka \leq 30$ [45]. In particular, it was found $\tau_k^s D k^2 \sim 1.08$ in good agreement with our result and $F_s(k, t)$ exhibits stretching with $\beta(k_{max}) \sim 0.8$.

The above findings agree with some predictions of MCT: i) T_c must be independent of the quantity under study, ii) γ_α must be equal to γ_D . The equality $\gamma_\alpha = \gamma_D$ must be taken with great caution. Other studies on the same model system with $N = 500$ and $P = 1$ found $\gamma_\alpha > \gamma_D$ even if fitting the diffusivity and τ_α provide the same T_c value [41].

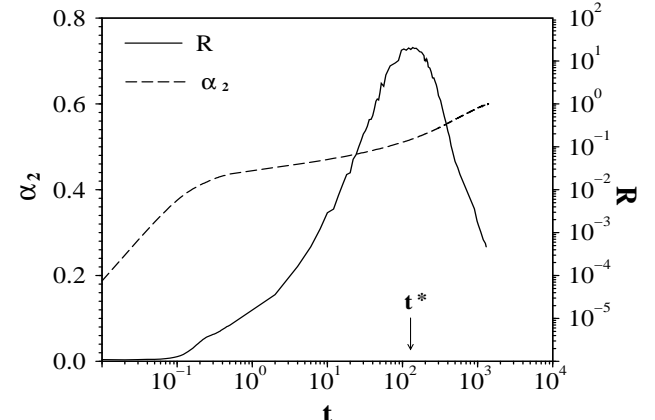


FIG. 8. Comparison of the non-gaussian parameter α_2 and the mean squared displacement $R(t)$ at $T = 0.5$. The maximum of the non-gaussian parameter occurs at t^* . t^* provides an estimate of the trapping time and is comparable with τ_α .

Additional information on the single-particle dynamics is provided by the self part of the Van Hove function $G_s(\mathbf{r}, t)$ [44]:

$$G_s(r, t) = \frac{1}{N} \left\langle \sum_{i=1}^N \delta(\mathbf{r} + \mathbf{R}_i(0) - \mathbf{R}_i(t)) \right\rangle \quad (9)$$

In isotropic liquids the Van Hove function depends only on the modulus r of \mathbf{r} . The interpretation of $G_s(r, t)$ is direct. The product $G_s(\mathbf{r}, t) \cdot 4\pi r^2$ is the probability that the molecule is at a distance between r and $r + dr$ from the initial position after a time t .

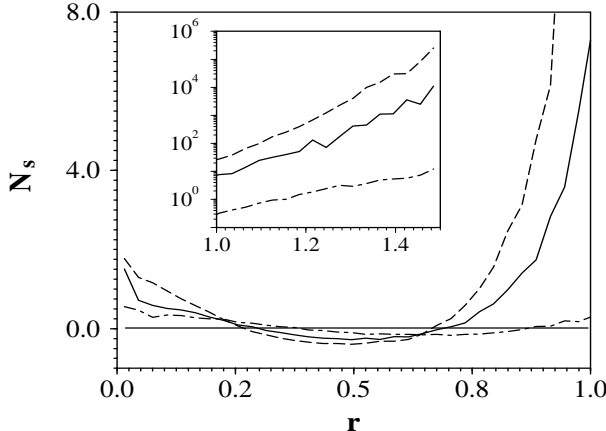


FIG. 9. The ratio $N_s(r) = (G_s(r, t^*) - G_s^g(r, t^*))/G_s^g(r, t^*)$ plotted at $T = 0.5$ (dashed line), $T = 0.588$ (solid line), $T = 0.85$ (dot-dashed line). Inset: same quantity on a logarithm scale.

The shape of $G_s(r, t)$ in the system under study does not reveal particular features [41]. In particular, differently from other studies [29], no secondary peak at $r \approx 1$, the nearest-neighbor distance, is found to support the conclusion that hopping is occurring. A deeper insight is gained by comparing $G_s(r, t)$ with the gaussian approximation:

$$G_s^g(r, t) = [3/2\pi\langle r^2(t) \rangle]^{3/2} \exp(-3r^2/2\langle r^2(t) \rangle) \quad (10)$$

Eq. 10 is the correct limit of $G_s(r, t)$ at short (ballistic regime, $\langle r^2(t) \rangle = 3kT/mt^2$) and long times (diffusion regime, $\langle r^2(t) \rangle = 6Dt$) [44]. Thirumalai and Mountain [28] and more recently Kob et al. [34] noted discrepancies between $G_s(r, t)$ and $G_s^g(r, t)$ in supercooled atomic mixtures. It is found that $G_s(r, t)$ exceeds $G_s^g(r, t)$ at short and long r values. The effect is particularly evident at $t \approx t^*$ where t^* is the time where the non-gaussian parameter

$$\alpha_2(t) = 3\langle r^4(t) \rangle/5\langle r^2(t) \rangle^2 - 1, \quad (11)$$

reaches the maximum value [41]. At t^* the stochastic properties of \mathbf{r} differ by the ones of a gaussian variable to the maximum. A plot of $\alpha_2(t)$ is shown in fig.8 where it is compared to the mean squared displacement $R(t)$ at $T = 0.5$. The maximum of $\alpha_2(t)$ at $t = t^*$ is located between the trapping and diffusive regimes. The decrease of $\alpha_2(t)$ for $t < t^*$ is due to the recovery of the gaussian form of $G_s(r, t)$ in the trapping regime where molecules undergo a nearly oscillatory motion in the cages where they are accommodated (fig. 2). t^* provides an estimate of the trapping time and in fact is comparable to the α -relaxation time. For $t \approx 0.2 - 0.3$, corresponding to the

second maximum of the velocity correlation function (fig.4), a small step is observed. The same feature of the non-gaussian parameter was observed in a MD work on a dense bidimensional liquid [46].

The deviations of the Van Hove function by the gaussian limit at short and long r values which were observed for $t \approx t^*$ shows that the sample has fractions of both trapped and highly mobile atoms [28,34]. It has been suggested that the dynamics of the latter is conveniently described by hopping processes [28]. To study the possible deviations of the Van Hove function in the present *molecular* system, we considered the ratio [34]:

$$N_s(r) = \frac{G_s(r, t^*) - G_s^g(r, t^*)}{G_s(r, t^*)} \quad (12)$$

Fig. 9 shows the ratio $N_s(r)$ for different temperatures. It exhibits increasing positive deviations at both short and large r values on cooling. This supports the conclusion that the dynamical heterogeneities evidenced in atomic two-phase systems are also present in *molecular* one-phase systems [28,34].

Non-vanishing $N_s(r)$ values could be anticipated by noting that the self-parts of the intermediate scattering function and the Van Hove function are related to each other by:

$$F_s(k, t) = \int_0^{+\infty} G_s(r, t) 4\pi r^2 \frac{\sin kr}{kr} dr \quad (13)$$

According to eq.13, the main contributions to $F_s(k_{max}, t)$ come roughly from $r < r^*$ with $r^* \approx 2\pi/k_{max} \approx 1$. If the discrepancies between $G_s(r, t^*)$ and $G_s^g(r, t^*)$ for $r < 1$ were small, $F_s(k_{max}, t) \approx \exp(-Dk_{max}^2 t)$ for $t \approx t^*$. Instead, $F_s(k_{max}, t)$ is found to decay as a stretched exponential (see fig.6 and related discussion).

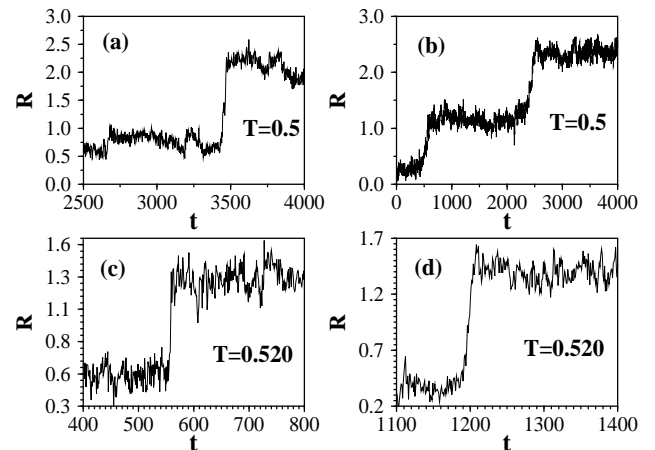


FIG. 10. Squared displacements R of selected molecules at $T = 0.5$ and $T = 0.520$. Note the distribution of the time needed to complete the jumps.

Since the positive tail of $N(r)$ at large r starts at $r \approx 1$ i.e. about the molecular size, it is tempting to ascribe it

to jump motion. Indeed, by inspecting the particle trajectories jumps are found. Examples are shown in fig. 10. It was noted that the jump duration exhibits a distribution (roughly between 20 – 500 time units), suggesting that different degrees of cooperativity are involved [35]. The translational jumps which are detected are relatively slower than the rotational jumps (flips of about 180°) which take about 6 – 7 time units with little or no distribution [38,39]. Furthermore, translational jumps are found to be much rarer than rotational ones [38]. In fact, differently from the translational case, the large amount of molecule flips manifests in a secondary peak of the proper Van Hove function [38,39,41].

The above remarks point to the conclusion that translational jumps are not obviously related to rotational ones. Their different character will be more clearly evidenced by studying and comparing the distributions of the waiting-times, i.e. the lapse of time between successive jumps (see below and ref. [38]).

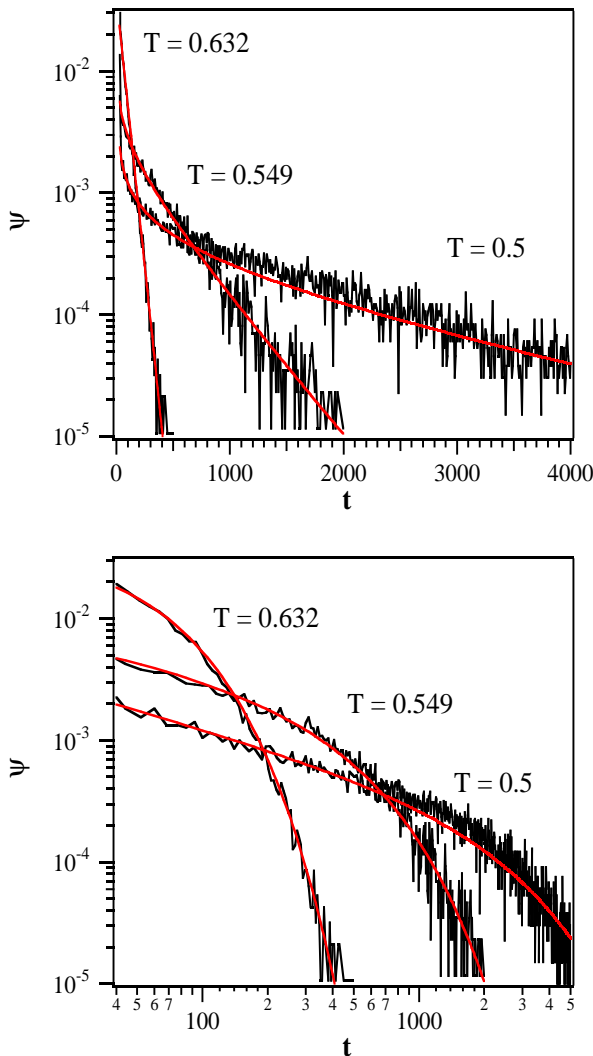


FIG. 11. Long-time (top) and short-time (bottom) behavior of the waiting-time distribution $\psi(t)$ at different temperatures. The solid lines superimposed to the curves is eq.14 with $\xi = 0.49$, $\tau = 2550$ ($T = 0.5$), $\xi = 0.63$, $\tau = 420$ ($T = 0.549$) and $\xi = 1$, $\tau = 49$ ($T = 0.632$).

The evaluation of the waiting-time distribution $\psi(t)$ relies on the explicit definition of a jump event. In the present study a molecule jumps at time t if the displacement between t and $t + \Delta t^*$ ($\Delta t^* = 24$) exceeds $\sqrt{\Delta R^*} = \sigma_{AA}/2 = 0.5$. To avoid multiple counting, the molecule which jumped at time t is forgotten up to time $t + \Delta t^*$. Possible spurious countings due to fast rattling motion are minimized by averaging each displacement with the previous and the next one. These are typically spaced by 6 – 8 time units, depending on the temperature [37]. It must be noted that after a time Δt^* the average diffusive displacement is smaller than ΔR^* , e.g. $\Delta R^{diff} = 6D\Delta t^* = 0.017$ at $T = 0.5$ and $\Delta R^{diff} = 0.032$ at $T = 0.520$. We validated the jump search procedure by inspecting several single-molecule trajectories. In particular, it was checked that molecular vibrations in local cages are not misinterpreted as jumps contributing to $\psi(t)$ at short-times. Some attempts to investigate how $\psi(t)$ depends on the above definition were made. Since they require wide statistics, the issue will not be touched in the present paper. It will be discussed in a more detailed way elsewhere.

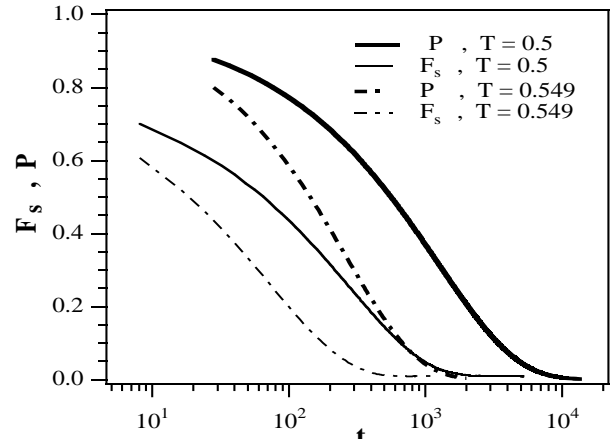


FIG. 12. Comparison between the probability that the waiting time between consecutive jumps is larger than t , $P(t)$, and $F_s(k_{max}, t)$ at $T = 0.5$ and 0.549 .

Fig.11 shows the waiting-time distribution $\psi(t)$ at different temperatures. At high temperature $\psi(t)$ is exponential. On cooling, the exponential decay is replaced at short times by a slowly-decaying regime. We fitted the overall decay by the function:

$$\psi(t) = [\Gamma(\xi)\tau^\xi]^{-1} t^{\xi-1} e^{-t/\tau} \quad 0 < \xi \leq 1 \quad (14)$$

The choice is motivated by the remark that in glassy systems rearrangements are rare events due to the constraints hampering the structural relaxation. It is be-

lied that intermittent behaviour in particle motion develops on cooling [33,47–49]. A signature of intermittence is the power law decay of $\psi(t)$ (for 2D liquids see [37]) and related quantities such as the first-passage time distribution [33]. The exponent ξ of eq.14 has a simple interpretation. If a dot on the time axis marks each relaxation event (a jump), the fractal dimension of the set of dots is ξ . For $\xi < 1$, it is found $\psi(t) \propto t^{\xi-1}$ at short times [47,50]. Modelling the long-time decay of $\psi(t)$ is less obvious. As a first guess, if the distribution of events becomes nearly uniform ($\xi = 1$) beyond a time scale τ and homogeneous across the sample, $\psi(t)$ recovers the exponential form.

The best fits at $T = 0.5, 0.549$ and 0.632 are shown in fig.11. The increase of temperature results in a weak increase of the exponent ξ and a more marked decrease of τ . It was found that eq.14 fits $\psi(t)$ also by setting $\sqrt{\Delta R^*}$ and Δt^* in the ranges $0.4 - 0.7$ and $24 - 48$, respectively. This suggests that the character of the decay of $\psi(t)$ is not strongly dependent on how a jump is defined. Nonetheless, the best fit values of the parameters ξ and τ depend on $\sqrt{\Delta R^*}$ and Δt^* differently. For example, at $T = 0.5$, if $\sqrt{\Delta R^*}$ changes from 0.5 to 0.6 with $\Delta t^* = 24$, ξ does not change within the errors whereas τ increases of a factor of about 2.4 . τ also increases by decreasing the time Δt^* allowed to perform the displacement $\sqrt{\Delta R^*}$. The increase of τ is understood by noting that increasing the threshold $\sqrt{\Delta R^*}$ or, alternatively decreasing Δt^* , reduces the number of sudden displacements which comply with the definition of "jump" and then increases the waiting time before a new jump occurs. Interestingly, at $T = 0.5$ $\psi(t)$ exhibits small but reproducible deviations from eq.14. They suggest that the long-time decay is *faster* than the exponential one. If the exponential decay is replaced by a gaussian one, the fit improves quite a lot and the ξ exponent changes from 0.49 to 0.45 . Even if this refinement is rather suggestive, we prefer to consider it as ad-hoc at the present level of understanding.

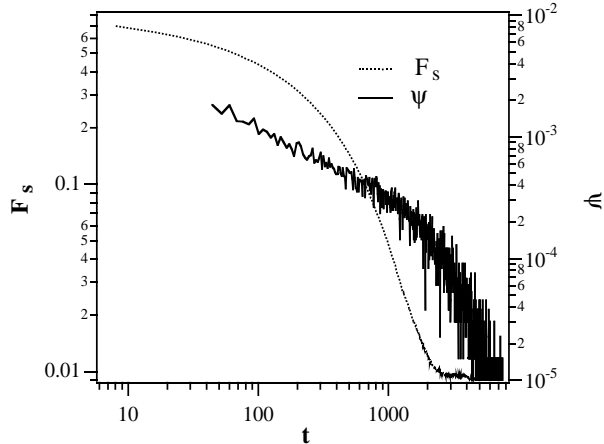


FIG. 13. Comparison between $\psi(t)$ and $F_s(k_{max}, t)$ at $T = 0.5$.

Further insight on $\psi(t)$ is offered by the study of the interplay between density fluctuations and the occurrence of jumps. This is of interest since, according to the extended version of MCT the dynamic transition occurring at T_c from an ergodic to a non-ergodic state is actually smeared by hopping processes [25]. Fig.12 compares at low temperatures the long-time tail of $F_s(k_{max}, t)$ and the probability that no jumps occurred before t , $P(t) = \int_t^\infty \psi(x) dx$. It is seen that the density self-correlations vanish at times when $P(t)$ is still meaningful (when $F_s(k_{max}, t) \sim 0.1$ $P(t) \sim 0.5$ at $T = 0.5$). There is also some evidence that the fraction of waiting times longer than the time needed to make $F_s(k_{max}, t)$ vanishing (e.g. $F_s(k_{max}, t) < 0.1$) increases on cooling. Strong analogies with the above findings are found in a recent MD work on the viscous silica melt [51]. It was reported that the probability that a bond between a silicon and an oxygen atom which was present at time zero is still present at time t vanishes much later than F_s even at high temperature.

Then, at lower temperatures two restructuring regimes are identified depending on the length of the waiting time with respect to τ_α . This is shown in fig. 13. For waiting times shorter than τ_α molecules jump in a nearly frozen environment. Escape from the cage becomes more difficult by lowering T and, expectedly, with a distribution of rates leading to the non-exponential decay of $\psi(t)$. For waiting times longer than τ_α a larger restructuring of the surrounding environment takes place. This averages the dynamical heterogeneities and leads to the long-time decay of $\psi(t)$.

It is tempting to note that in the time window where $\psi(t)$ exhibits the power law decay MCT predicts that $F_s(k, t)$ itself decays as the von Schweidler power law [25]:

$$F_s(k, t) = f_s^c(k) - h^s(k) \left(\frac{t}{\tau}\right)^b + \dots \quad (15)$$

where $f_s^c(k)$, $h^s(k)$ and b are constants. $F_s(k_{max}, t)$ must be compared to $P(t) \approx A - Bt^\xi + \dots$ in the region of interest. A and B are constants. If one estimates b via the β parameter of the stretched exponential fit of the long-time decay of $F_s(k_{max}, t)$, it is found $b \cong \beta = 0.68$ at $T = 0.5$. This must be compared to $\xi = 0.45$. To make clearer to what extent the two time fractals are related to each other the analysis should be refined [41]. This is beyond the purposes of the present paper. However, we note that for times shorter than about $\Delta t^* = 24$ $\psi(t)$ and then $P(t)$ cannot be defined since most jumps are not completed.

C. Collective dynamics: the shear viscosity

The shear viscosity η was evaluated by using the Einstein relation [52]:

$$\eta = \frac{1}{2VkT} \lim_{t \rightarrow +\infty} \frac{1}{t} \langle \Delta A(t)^2 \rangle \quad (16)$$

where:

$$\Delta A(t) = V \int_0^t \mathcal{P}_{\alpha\beta}(t') dt' \quad (17)$$

$\mathcal{P}_{\alpha\beta}$ is one off-diagonal component of the pressure tensor [44,52,53] (in practice $\Delta A(t)$ is the average over the three possible choices $\alpha\beta = xy, xz, yz$).

If the quantity $\mathcal{P}_{\alpha\beta}V$ is evaluated based on the motion of individual atoms comprising the molecules in the system we have [54]

$$\mathcal{P}_{\alpha\beta}^{at}(t)V = \sum_{i=1}^N m_i v_{i\alpha} v_{i\beta} + \sum_{i=1}^N \sum_{j>i}^N f_{\alpha ij}(r_{i\beta} - r_{j\beta}) \quad (18)$$

The sums involve components (denoted by greek letters) of \mathbf{v}_i , \mathbf{r}_i and \mathbf{f}_{ij} which are the velocity and the position of the i -th atom having mass m_i and the force between the atoms i and j (assumed pairwise additive), respectively. Eq.18 is not affected by the periodic boundary conditions employed in MD simulations.

An interesting alternative to the above atomic representation of the pressure tensor is the molecular one which replaces $\mathcal{P}_{\alpha\beta}^{at}$ with the symmetric part of the tensor [54]

$$\mathcal{P}_{\alpha\beta}^{mol}(t)V = \sum_{i=1}^N M_i V_{i\alpha} V_{i\beta} + \sum_{i=1}^N \sum_{j>i}^N F_{\alpha ij}(R_{i\beta} - R_{j\beta}) \quad (19)$$

The sums now involve components of \mathbf{V}_i , \mathbf{R}_i and \mathbf{F}_{ij} which are the centre-of-mass velocity and the centre-of-mass position of the i -th molecule having mass M_i and the total force between the molecules i and j , respectively. Evaluating the atomic pressure tensor via eq.18 is a little more efficient than the alternative one and was adopted in the present study. Nonetheless, we found that the two representations exhibit the same convergence when evaluating eq.16 and yield identical results in agreement with previous studies [55].

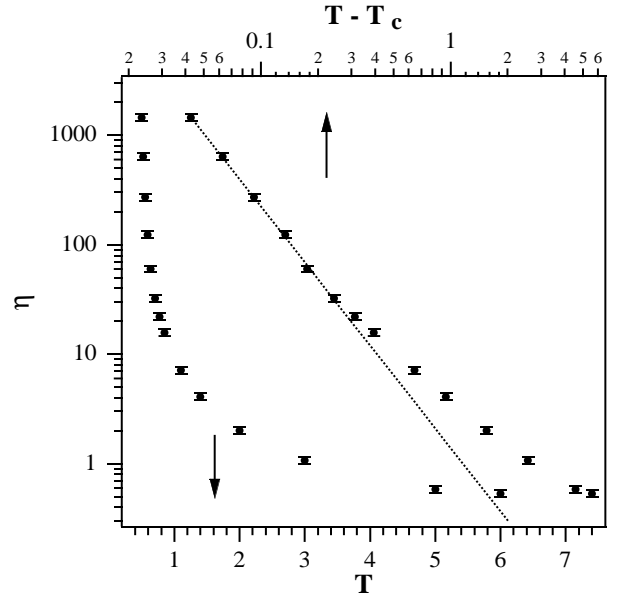


FIG. 14. Temperature dependence of the shear viscosity. The superimposed line has slope $\gamma_\eta = -2.20 \pm 0.03$.

The evaluation of the shear viscosity is particularly time-consuming being a collective property which involves many-particle correlations. In fact, if one evaluates a generic N -particle property by a run spanning a time interval as long as t , the relative error r is of the order of $(\tau_c/t)^{1/2}$, τ_c being the correlation time. The error is quite larger than the one of a single-particle property which is of the order of $2(\tau_c/Nt)^{1/2}$ [42,56]. Then, long runs are needed to reach sufficient statistics. However, the specific case of the viscosity is less dramatic. In supercooled liquids the viscosity is roughly proportional to the longest relaxation time of $F(k, t)$, the coherent intermediate scattering function, which occurs at $k \cong k_{max}$ [41]. In particular, for moderately supercooled liquids a mode-coupling theory shows that η is given by [57]:

$$\eta = \frac{kT}{60\pi^2} \int dt \int dk V^2(k) \left[\frac{F(k, t)}{S(k)} \right]^2 \quad (20)$$

where $V(k) = k^2 d \ln S(k) / dk$. The vertex $V(k)$ greatly reduces the weight of hydrodynamic wave vectors. The main contributions to the above integral are due to modes being located around k_{max} with a spread $|k_{max} - k|/\Delta \sim 1.4$, Δ is the half-width of the main peak of $S(k)$, whose inverse being a measure of the extent of correlations in direct space [57]. Then, for a sample of volume V the relative error of η is decreased with respect to the above estimate by an additional factor $(v/V)^{-1/2}$, with $v = \Delta^{-3}$ [56]. In order to have runs longer than the relaxation time of $F(k_{max}, t)$ and keep reasonable execution times V must be small. On the other hand V must be larger than v . We chose samples accommodating $N = 108$ molecules and carried out runs as long as $40t^*$ at least, t^* being the time when $F_s(k_{max}, t)$ vanishes (i.e. when it drops below 0.02). t^* provides an estimate of the time scale to reach

the limit in eq.16. At the lowest temperature, $T = 0.5$, the volume was $V \sim 150$ and $v \sim 8$. Consequently, the relative error of the viscosity $2(v\tau_c/Vt)^{1/2}$ is estimated to be about 7%. This figure was confirmed by collecting several runs at each temperature. We also explicitly tested that the viscosity of small ($N = 108$) and large samples ($N = 1000$) at $T = 0.7$ exhibits no significant difference.

Small samples to evaluate η in supercooled systems were also used by Thirumalai and Mountain [28].

In Fig. 14 the shear viscosity is shown as a function of the temperature. It covers a range of more than three orders of magnitude. The data are also plotted as function of $\log(T - T_c)$ evidencing that the viscosity, differently from the diffusivity, may not be described by a power law analogous to eq.7 in the overall temperature range investigated. If the fit with a power law analogous to eq.7 is limited to $T < 0.85$, it is found $\gamma_\eta = -2.20 \pm 0.03$.

D. The Stokes-Einstein law

Several experimental [3,4,7–9,11,13] and numerical [20,24,28–30,33] works evidenced a decoupling of the translational diffusion and the viscosity on approaching the glass transition. Typically, the decoupling occurs around T_c [3]. To date, MD investigated the issue in one- and two-components *atomic* systems. It is therefore of interest to examine the present molecular system from that respect.

The decoupling manifests as an enhancement of the translational diffusion D with respect to the prediction of the Stokes-Einstein relation (SE) which reads [58]

$$D = \frac{kT}{\eta\mu} \quad (21)$$

μ is a constant that depends on both the molecule geometry and the boundary conditions. For a sphere of radius a , μ equals $6\pi a$ or $4\pi a$ if stick or slip boundary conditions occur, respectively. The problem of uniaxial ellipsoids in the presence of stick boundary conditions may be worked out analytically [58]. Tables of μ for prolate ellipsoids with slip boundary conditions were also reported [59]. The case of the biaxial ellipsoid with stick boundary condition was discussed recently by noting an interesting electrostatic analogy [60].

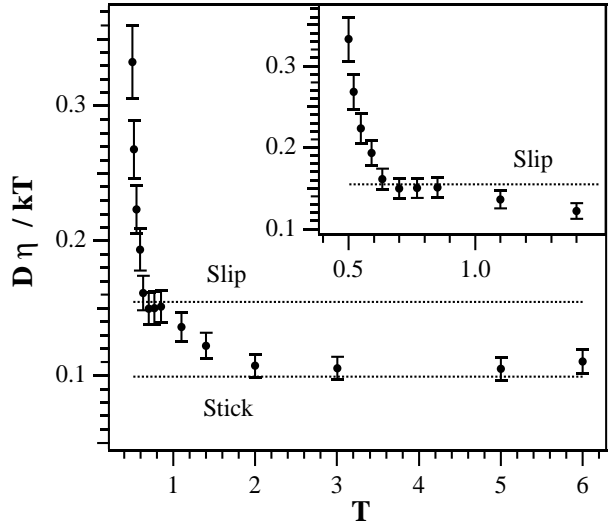


FIG. 15. The temperature dependence of the ratio $D\eta/kT$. SE predicts a constant value. Dashed lines are the SE predictions for prolate ellipsoids with semiaxis $b = 0.46$ and $c = 0.69$ and stick or slip boundary conditions. A magnification of the low- T region is shown in the inset.

In Fig. 15 we plot the ratio $D\eta/kT$ as a function of temperature. According to SE the ratio must be constant. At higher temperatures the ratio levels off at about 0.105 ± 0.007 . On cooling, there is first a mild change followed by a steep increase below $T = 0.632 = 1.38T_c$.

It is believed that the SE failure is a signature of the heterogeneous dynamics of supercooled liquids [16–19]. Alternative views are provided by frustrated lattice gas models [20] and the “energy landscape” picture [2,21–24]. Most interpretations suggest the existence of crossover temperatures broadly located around T_c [3]. From this respect it is tempting to note that the SE law breaks down at $T \sim 0.632$ below which intermittent behavior evidences (see fig.11). Intermittence disappears for times longer than τ_α (see fig. 13) which is consistent with a growing dynamic heterogeneity of the liquid.

Around $T = 0.77$ a plateau at 0.151 ± 0.01 is reached. We have compared the results to the prediction of the SE law for prolate ellipsoids. The diatomic molecule under study may be roughly sketched as a prolate ellipsoid with semiaxis $b = 3/4$ and $c = 1/2$. The corresponding ratio $D\eta/kT$ for stick and slip boundary conditions is equal to 0.091 and 0.1415, respectively. The values compare well to the high- and low- T plateau which are observed in fig.15. By setting $b = 0.69$ and $c = 3/2b$ the agreement is improved with $D\eta/kT = 0.098$ and 0.154 for stick and slip boundary conditions, respectively. The above analysis provides reasonable evidence of a precursors effect of the SE breakdown which manifests itself as an apparent stick-slip transition. A quite similar crossover from stick to slip boundary conditions has been observed on approaching the glassy freezing of colloidal suspensions [61]. Since we are studying a one-component system, the effect seems to be conceptually different by the apparent change of the boundary conditions which has been evi-

denced by a recent MD study of the motion of a guest tracer in a liquid host [62].

It is worthwhile to mention that the SE law evidences fine modifications of the supercooled liquid behavior which are hardly found by inspecting the diffusivity. The latter exhibits a single power-law regime over all the temperature range we studied.

IV. CONCLUSIONS

The transport and the relaxation properties of a molecular supercooled liquid on the isobar $P = 1.5$ has been studied by molecular dynamics. The molecule is a rigid A-B system. On cooling, the diffusivity decrease is fitted over four orders of magnitude by the power law $D \propto (T - T_c)^{\gamma_D}$ with $\gamma_D = 1.93 \pm 0.02$ and $T_c = 0.458 \pm 0.002$. The divergence of the primary relaxation time τ_α drawn by the intermediate scattering function $F_s(k_{max}, t)$ tracks the diffusivity at the lowest temperatures according to $\tau_\alpha \propto (k_{max}^2 D)^{-1}$. The result confirms findings on hard sphere systems [45]. It disagrees with other studies on the same model system under study here which noticed that a power-law fit of D and τ_α yields the same T_c value but $\gamma_\alpha > \gamma_D$ with $N = 500$, $P = 1$ [41].

At the lowest temperatures fractions of highly mobile and trapped molecules are evidenced, then extending previous results on supercooled atomic mixtures to one-component molecular liquids [28,34]. Translational jumps are evidenced. The duration of the jumps exhibits a distribution. The distribution of the waiting-times before a new jump takes place, $\psi(t)$, is exponential at higher temperatures. At lower temperatures two regimes are evidenced: at short times $\psi(t) \propto t^{\xi-1}$ with $0 < \xi \leq 1$ whereas at long times the decay is faster than exponential. The crossover between the two regimes occurs around τ_α . Noticeably in this time window MCT predicts that $F_s(k_{max}, t)$ also decays as a power law. The interplay between the two time fractals is anticipated and a preliminary analysis has been attempted. The fractal distribution of the waiting time is ascribed to the intermittent behavior which is expected to develop in glassy systems [47–49,33]. If the waiting time before a new jump exceeds τ_α the environment surrounding each molecule largely restructures. The subsequent average process results in a faster decay of $\psi(t)$. The probability that no jump occurred before time t is found to vanish slower than $F_s(k_{max}, t)$ in close analogy with the case of viscous silica melts [51].

The shear viscosity has been studied over more than three orders of magnitude. The data are fitted by the power law $\eta \propto (T - T_c)^{\gamma_\eta}$ with $\gamma_\eta = -2.20 \pm 0.03$ at the lowest temperatures. The validity of the Stokes-Einstein relation has been examined. Previous MD studies were limited to atomic one- and two- components systems. At higher temperatures SE fits well the data if *stick* boundary conditions are assumed. At lower temperatures the

product $D\eta/T$ increases and the Stokes-Einstein relation is not obeyed. The breakdown occurs near to the temperature where the intermittency is evidenced by $\psi(t)$. Interestingly, a precursor effect of the breakdown is observed which manifests as an apparent stick-slip transition. A crossover from stick to slip boundary conditions has been observed on approaching the glassy freezing of colloidal suspensions [61].

ACKNOWLEDGMENTS

The authors warmly thank Walter Kob for having suggested the investigation of the present model system, the careful reading of the manuscript and the comments on it. Umberto Balucani, Claudio Donati and Francesco Sciortino are thanked for many helpful discussions and Jack Douglas for a preprint of ref. [33].

APPENDIX A: RATTLE-NPT ALGORITHM

The well-known Nosè-Andersen algorithm ensures NPT equilibrium, i.e. equilibrium at constant number of particles, pressure P and temperature T [42]. It defines one extra degree of freedom $s(t)$, describing the thermal bath and allows the change of the volume $V(t)$. Since the algorithm was originally derived for atoms, the extension to molecules is of interest. To this aim, the so-called constraint methods are of help, particularly the RATTLE algorithm [42]. It evaluates the dynamics of polyatomic molecules by defining proper forces constraining the relative motion of the atoms belonging to the same molecule. Below, the combined RATTLE-NPT algorithm is described.

First, the vector $\mathbf{R}(t + \delta t)$ of all atoms positions, $s(t + \delta t)$ and the vector $\mathbf{V}(t + \delta t)$ of all atoms velocities and the their first time derivatives at mid-step $\mathbf{V}(t + \delta t/2, \dot{s}(t + \delta t/2))$, $\dot{\mathbf{V}}(t + \delta t/2)$ are evaluated according to the RATTLE algorithm. The forces $\mathbf{f}_i(t + \delta t)$ (i refers to the i -th atom) are expressed in terms of the configuration $\mathbf{R}(t + \delta t)$. The other steps are the following:

1. Guess of the first derivatives of interest at time $t + \delta t$, $\dot{\mathbf{y}}^g(t + \delta t)$ ($\dot{\mathbf{y}} = \mathbf{v}, \dot{s}, \dot{\mathbf{V}}$) :

$$\dot{\mathbf{y}}^g(t + \delta t) = 2\dot{\mathbf{y}}(t) - \dot{\mathbf{y}}(t - \delta t)$$

The above guess, which is correct to second order, is not unique and alternatives are possible.

2. Calculation of temperature $T(t + \delta t)$ by using $\mathbf{v}^g(t)$.
3. Calculation of $\dot{s}(t + \delta t)$. Replacing the lagrangian equation for $\ddot{s}(t + \delta t)$ into the velocity Verlet equations [42] yields:

$$\dot{s}(t + \delta t) = A + \frac{A^2}{s} \delta t + \frac{A^3}{2s^2} \delta t^2 + O(\delta t^3),$$

with $A = s(t + \frac{1}{2}\delta t) + \frac{1}{2}\delta t f \frac{T(t + \delta t) - T_0}{Q} s(t + \delta t)$. Q , T_0 and f are the mass of the thermal piston, the thermal bath temperature and the degrees of freedom ($f = \frac{5}{2}N_{at} - 3$ in the present case), respectively.

4. Calculation of pressure $P(t + \delta t)$.
5. Evaluation of $\dot{V}(t + \delta t)$ according to the velocity Verlet algorithm:

$$\begin{aligned} \dot{V}(t + \delta t) = \\ \frac{\dot{V}(t + \frac{1}{2}\delta t) + \frac{1}{2}\delta t \frac{s^2(t + \delta t)}{W} (P(t + \delta t) - P_0)}{1 - \frac{1}{2}\delta t \dot{s}(t + \delta t)/s(t + \delta t)} \end{aligned}$$

where W and $P(t)$ are the mass of the piston setting the pressure at P_0 and the instantaneous pressure, respectively.

6. Evaluation of the velocities at time $t + \delta t$, $\mathbf{v}_i(t + \delta t)$ in the presence of the intermolecular forces, the thermal bath forces and the forces due to the mechanical piston. According to the velocity Verlet algorithm:

$$\begin{aligned} \mathbf{v}_i(t + \delta t) = (1 + \frac{1}{2}\delta t \dot{s}(t + \delta t)/s(t + \delta t))^{-1} \times \\ \left\{ \mathbf{v}_i(t + \frac{1}{2}\delta t) + \frac{1}{2}\delta t \mathbf{f}_i(t + \delta t) + \right. \\ \left. \frac{1}{2}\delta t \left[\frac{\ddot{V}}{3V} + \left(\frac{\dot{s}}{s} - \frac{2}{3} \frac{\dot{V}}{V} \right) \frac{\dot{V}}{3V} \right] \mathbf{R}_{cm,i} \right\} \end{aligned}$$

where $\mathbf{R}_{cm,i}$ is the center of mass of the molecule where the i -th atom is located.

7. Adjustment of the velocity \mathbf{v}_i . The relative velocities of atoms which are mutually bonded are considered and their component along the bond is made to vanish, according to the RATTLE algorithm.

Finally we note that iterating steps from 2 through 7 increases the accuracy considerably. The present algorithm needs to store the arrays $\mathbf{V}(t - \delta t)$, $\dot{s}(t - \delta t)$ and $V(t - \delta t)$ to guess the velocity as $v^g(t + \delta t)$ in the first step.

- [1] Proceedings of the II Workshop on Non-Equilibrium Phenomena in Supercooled Fluids, Glasses and Amorphous Materials, M.Giordano, D.Leporini, M.P.Tosi (eds.). *J.Phys.:Condens.Matter*, Vol.11, No.10A (1999).
- [2] for a short review see: M.D.Ediger, C.A.Angell, S.R.Nagel *J.Phys.Chem* **100**, 13200 (1996);
- [3] E. Rössler, *Phys.Rev.Lett.* **65**, 1595 (1990).
- [4] F. Fujara, B.Geil, H.Sillesscu, G.Fleischer *Z.Phys.* **B88**, 195 (1992); I.Chang, F.Fujara, B.Geil, G.Heuberger, T.Mangel, H.Sillesscu *J.Non-Cryst.Solids* **172-174** 248 (1994).
- [5] E. Rössler, J.Tauchert, P.Eiermann *J.Phys.Chem.* **98**, 8173 (1994).
- [6] E. Rössler, P.Eiermann *J.Chem.Phys.* **100**, 5237 (1994).
- [7] M.T. Cicerone, F.R.Blackburn, M.D.Ediger *J.Chem.Phys.*, **102**, 471 (1995); M.T. Cicerone, M.D.Ediger *J.Chem.Phys.*, **104**, 7210 (1996).
- [8] J.C.Hooker, J.M.Torkelson *Macromolecules*, **28**, 7683 (1995).
- [9] G.Heuberger, H.Sillesscu *J.Phys.Chem.*, **100**, 15255 (1996).
- [10] J.Y.Ye, T.Hattori, H.Nakatsuka, Y.Maruyama, M.Ishikawa, *Phys.Rev.B* **56**, 5286 (1997).
- [11] D.B.Hall, A.Dhinojwala, J.M.Torkelson *Phys.Rev.Lett.* **79**, 103 (1997).
- [12] L.Andreozzi, A.Di Schino, M.Giordano, D.Leporini, *Europhys.Lett.* **38**, 669 (1997).
- [13] A.Voronel, E.Veliyulin, V.Sh.Machavariani, A.Kisliuk, D.Quitmann *Phys.Rev.Lett.* **80**, 2630 (1998).
- [14] M.Faetti, M.Giordano, L.Pardi, D.Leporini *Macromolecules*, **32**, 1876 (1999).
- [15] L.Andreozzi, M.Faetti, M.Giordano, D.Leporini *J.Phys.Chem.B* **103**, 4097 (1999).
- [16] J. A. Hodgdon, F. H. Stillinger *Phys.Rev.E* **48**, 207 (1993); F. H. Stillinger, J. A. Hodgdon *ibid.* **50**, 2064 (1994);
- [17] C.Z.-W. Liu, I.Oppenheim, *Phys.Rev.* **E53**, 799 (1996).
- [18] J.F.Douglas, D.Leporini *J.Non-Cryst.Solids* **235-237**, 137 (1998).
- [19] H.Sillesscu *J.Non-Cryst.Solids* **243**, 81 (1999).
- [20] M. Nicodemi, A. Coniglio, *Phys. Rev. E* **56**, R39 (1998); A.Coniglio, A.DeCandia, A.Fierro, M. Nicodemi *J.Phys.:Condens.Matter*, **11**, A167 (1999).
- [21] M.Goldstein *J. Chem. Phys.* **51**, 3728 (1969);
- [22] S.Sastry, P.G.Debenedetti, F.H.Stillinger *Nature* **393**, 554 (1998);
- [23] C.A.Angell *J.Res.Natl.Inst.Std.Tech.*, **102**, 171 (1997); C.A.Angell, B.E.Richards, V.Velikov *J.Phys.:Condens.Matter*, **11**, A75 (1999).
- [24] L.Angelani, G.Parisi, G.Ruocco, G.Viliani *Phys.Rev.Lett.* **81**, 4648 (1998).
- [25] W.Götze *J.Phys.:Condens.Matter*, **11**, A1 (1999); H.Z.Cummins *J.Phys.:Condens.Matter*, **11**, A95 (1999).
- [26] T.Franosch, W.Götze *Phys. Rev. E* **57**, 5833 (1998).
- [27] W.Kob, *J.Phys.:Condens.Matter* **11** R85 (1999).
- [28] D.Thirumalai, R.D.Mountain *Phys. Rev. E* **47**, 479 (1993).
- [29] J.-L.Barrat, J.-N.Roux, J.P.Hansen *Chem.Phys.*, **149**,

* corresponding author: e-mail address:
leporini@mailbox.difi.unipi.it.

197 (1990).

[30] R.Yamamoto, A.Onuki *Phys. Rev. E* **58**, 3515 (1998).

[31] R.Yamamoto, A.Onuki *Phys. Rev. Lett.* **81**, 4915 (1998).

[32] D.Perera and P.Harrowell *Phys. Rev. Lett.* **81**, 120 (1998).

[33] P.Allegrini, J.F.Douglas, S.H.Glotzer submitted to *Phys.Rev.E*

[34] W.Kob, C.Donati, S.J.Plimpton, P.H.Poole, S.C.Glotzer *Phys.Rev.Lett.* **79** 2827 (1997); C.Donati, J.F.Douglas, W.Kob, S.J.Plimpton, P.H.Poole, S.C.Glotzer *Phys.Rev.Lett.* **80** 2338 (1998).

[35] H.Miyagawa, Y.Hiwatari, B.Bernu, J.P.Hansen, *J.Chem.Phys.* **88**,3878 (1988);

[36] G.Wahnström, *Phys.Rev.A*, **44**, 3752 (1991).

[37] T.Muranaka, Y.Hiwatari, *J.Phys.Soc of Japan*, **67** 1982 (1998).

[38] C.De Michele, D.Leporini submitted to *Phys. Rev. E*.

[39] S.Kämmerer, W.Kob, R.Schilling *Phys.Rev.E* **56** 5450 (1997).

[40] S.Kämmerer, W.Kob, R.Schilling *Phys.Rev.E* **58** 2141 (1998).

[41] S.Kämmerer, W.Kob, R.Schilling *Phys.Rev.E* **58** 2131 (1998).

[42] M.P.Allen, D.J.Tildesley *Computer Simulation of Liquids* (Clarendon Press, Oxford 1987)

[43] S.Kämmerer, W.Kob, R.Schilling, private communication

[44] J.-P.Hansen, I.R. McDonald *Theory of Simple Liquids* II Edition (Academic Press, London 1986).

[45] M.Fuchs, I.Hofacher, A.Latz *Phys.Rev A***45** 898 (1992).

[46] M.M.Hurley, P.Harrowell *J.Chem.Phys.***105** 10521 (1996).

[47] L.Sjögren *Z.Phys.B* **74**, 353 (1989).

[48] J.F.Douglas, J.B.Hubbard *Macromolecules* **24**, 3163 (1991); J.F.Douglas *Comp.Mat.Sci.* **4**, 292 (1995).

[49] T.Odagaki *Phys.Rev.Lett.* **75**, 3701 (1995).

[50] R.Hilfer, L.Anton *Phys.Rev.E* **51**, R848 (1995).

[51] J.Horbach, W.Kob *Phys.Rev.B* **60**, 3169 (1999).

[52] M.P.Allen, D.Brown, A.J.Masters *Phys.Rev.E* **49** 2488 (1994).

[53] In principle, the viscosity η may be also evaluated by a proper Green-Kubo relation involving the area below the self-correlation function of the off-diagonal components of the pressure tensor $\mathcal{P}_{\alpha\beta}$, $\eta(t)$ [44,52]. However, the slowly-decaying tail of $\eta(t)$ poses numerical problems [29,42,44].

[54] M.P.Allen *Mol.Phys.* **52** 705 (1984).

[55] S.T.Cui, P.T.Cummings, H.D.Cochran *Mol.Phys.* **88** 1657 (1996).

[56] D.Frenkel in Proceedings of the International School of Physics "Enrico Fermi", Vol. 75 (Soc. Italiana di Fisica, Bologna 1980).

[57] U.Balucani, *Mol.Phys.* **71** 123 (1990); S.Bhattacharyya, B.Bagchi *J.Chem.Phys.* **109**,7885 (1998).

[58] H.Lamb *Hydrodynamics* VI Ed. (Cambridge University Press, Cambridge 1932).

[59] S.Tang, G.T.Evans *Mol.Phys.* **80** 1443 (1993).

[60] J.B.Hubbard, J.F.Douglas, *Phys.Rev.E* **47**, R2983 (1993).

[61] P.N.Segre', S.P.Meeker, P.N.Pusey, W.C.K.Poon *Phys.Rev.Lett.* **75**, 958 (1995).

[62] G.Srinivas, S.Bhattacharyya, B.Bagchi *J.Chem.Phys.* **110**, 4477 (1999).